Journal of Autonomous Intelligence (2024) Volume 7 Issue 4
doi: 10.32629/jai.v7i4.1461

ORIGINAL RESEARCH ARTICLE

Silicon retina: Focusing on motion studies for detecting the *x*-axes and *y*-axes

Zekun Li[1,*], Tiankuo Jiao[2]

[1] *University of Edinburgh, Electronic, Fountainbridge Scotland EH3 9QG, Britain*

[2] *University of Cambridge, Engineering, Cambridge CB2 1PZ, Britain*

*** Corresponding author:** Zekun Li, sgzli51@163.com

ABSTRACT

The purpose of this report is to explore how to build a circuit that works as a human retina, which can detect motion. The whole project is divided into five steps, which include researching, simulating, building a cell on the breadboard and testing, presenting a cell on Printed Circuit Board and testing, printing more cells, and connecting all the cells. Through each step of the execution, the output signals from the *x*-axis and *y*-axis become more and more accurate, in other words, the speed measured by the entire retinal system becomes more and more accurate. When connecting the photoreceptor as the input, different motion types, which include moving fast or slow, moving horizontally or vertically, and moving upward at an angle or downward at an angle, and the results are also basically following the analysis and the expected result read from the books or journals. The errors are mainly caused by the different light conditions in the environment.

Keywords: silicon retina; aperture problem; constraint-solving circuit; cell; phototransistor

ARTICLE INFO

Received: 27 November 2023
Accepted: 21 December 2023
Available online: 25 January 2024

1. Introduction

1.1. Objectives

The purpose of this project is to explore the silicon retina. The main task of this project is to focus on one of the functions of the human retina, which is detecting motion in the *x*-axis and *y*-axis directions from the real world. In other words, this project is to build a circuit to measure the speed of the motion in the *x* direction and *y* direction. This is very similar to an optical motion sensor, which uses different photodiodes to receive and transmit the light intensity and then calculate the velocity of the motion[1].

1.2. Theoretical background

1.2.1. The silicon retina

The silicon retina, which is defined as a silicon chip or a large-scale integrated circuit that performs the functions of the neural circuitry of a real retina in human eyes[2]. For the real retina of a human, it is a thin sheet of tissue that partially lines the orb of the eye. This tiny issue in human's eyes is able to collect all the visual information from the world and convert the visual information such as raw light into a signal that can reach to the human's brain to be processed[3]. Silicon retina is similar to image processing systems, which is defined that a combination system that can receive light signal from the environment, processing the received signal, transform images into digital form and get some useful information by performing certain operations[3]. In this project, the main task of this project is to focus on the function of detecting motion in the *x*-axis and *y*-axis directions from the real world.

1.2.2. Aperture problem

Local motion information from a single neuron is inherently ambiguous for global motion. That is, many different motions in the retina can elicit the same response in a single motion-sensitive neuron with a small receptive field. This is known as the aperture problem[4]. To be simpler, when the field of view is limited, an inherent ambiguity will occur. For example, according to **Figure 1**, there is a long bar whose length is larger than the diameter of a small circle aperture moving horizontally to the dashed line, however, the real velocity of the motion cannot be uniquely determined through a small aperture, because the real direction of the motion cannot be determined caused by the limited field of view, thus there are infinite family of possible velocities, as illustrated by the arrows. The image velocity components V_x and V_y can be regarded as the *x* and *y* coordinate in a velocity plane. All the possible velocities can be drawn in this plane and form a line called constraint line, shown in **Figure 1**. Many of the motion-sensitive neurons in the visual system, especially those early in the visual system, tend to have relatively small receptive fields. That is, they respond to only a small part of the retina. They can only respond to the motion within or in the receptive area. Such neurons provide information about ‘local’ motion. Later in the visual system, information from several neurons that respond to local movements in similar parts of the retina is integrated, allowing us to perceive the whole, or overall movement, of an image[4].

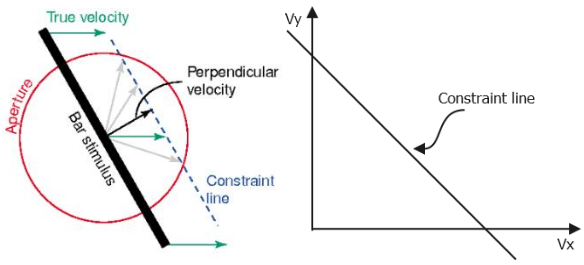

(a) **(b)**

Figure 1. (a) the aperture problem; **(b)** the constraint line[4].

1.2.3. Constraint-solving circuit

In order to solve the aperture problem and get the real speed of the motion, light intensity can be used. According to **Figure 2**, the different speed of motions results in different changes in light intensity, thus the real velocity of the motion can be determined by the light intensity. The relationship between light intensity and velocity is following the Horn and Schunk equation[5]:

$$\frac{\partial I}{\partial x}V_x + \frac{\partial I}{\partial y}V_y + \frac{\partial I}{\partial t} = 0\# \tag{1}$$

where *I* is the light intensity, V_x is the velocity in the x coordinate, V_y is the velocity in the y coordinate, $\partial I/\partial t$ is the change in light intensity with time, $\partial I/\partial x$ is the change in light intensity with the velocity in the *x* coordinate, and $\partial I/\partial y$ is the change in light intensity with the velocity in the y coordinate. Based on the equation, three derivatives of the intensity do not allow velocity to be determined uniquely, thus there is an inherent ambiguity. To be more specific, there are two variables in one equation, which means there are infinite possible solutions for this equation[5].

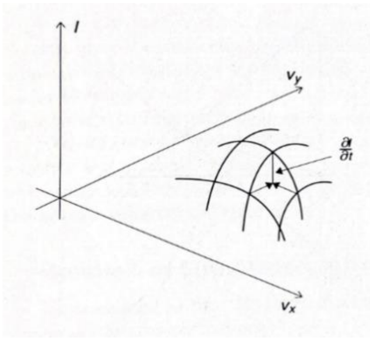

Figure 2. The light intensity surface on velocity plane[5].

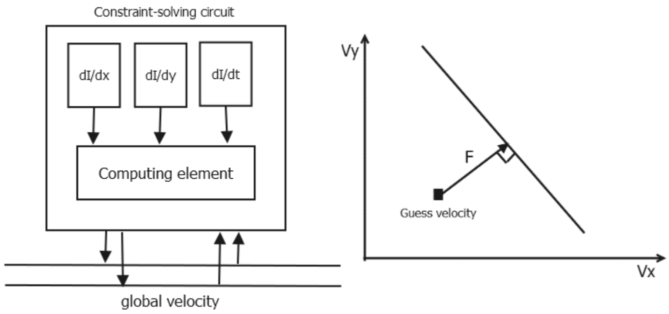

(a) **(b)**

Figure 3. (a) the correction force[5]; **(b)** the constraint-solving circuit[5].

In order to solve the Horn and Schunk equation, a constraint-solving circuit (**Figure 3**), which is also called a cell, is supposed to be used. Specifically, the first step is that a set of global wires distributes a best guess to all the individual sites, next, check error between global velocity and the constraint line, and finally, supplying a force to move global velocity onto the constraint line to satisfy the local constraint (The correction force is always perpendicular to the line, which is shown in **Figure 3**). The mathematical process of how the constraint-solving circuit solves the Horn and Schunk equation is shown below (The derivation of correction force). Firstly, converting the Horn and Schunk equation into the slope intercept form.

$$V_y = -\frac{\partial I/\partial x}{\partial I/\partial y} * V_x - \frac{\partial I/\partial t}{\partial I/\partial y} \tag{2}$$

Thus, the slope of the constraint line, where defined, is[5]

$$m = -\frac{\partial I/\partial x}{\partial I/\partial y} \tag{3}$$

Because the correction force is always perpendicular to the constraint line, the slope of the correction force is

$$Fslope = -\frac{1}{m} = -\frac{\partial I/\partial y}{\partial I/\partial x} \tag{4}$$

Thus, a unit vector in the direction of correction force is

$$\frac{\nabla I}{|\nabla I|} = \left\langle \frac{\partial I/\partial x}{\sqrt{(\partial I/\partial x)^2 + (\partial I/\partial y)^2}}, \frac{\partial I/\partial y}{\sqrt{(\partial I/\partial x)^2 + (\partial I/\partial y)^2}} \right\rangle \tag{5}$$

Because the forcing function is linear with error distance, which means the magnitude of the force is increasing with the increase in the distance between constraint line and guessed global velocity point, the forcing function can be computed as[5]

$$D = -\frac{\frac{\partial I}{\partial x}V_x + \frac{\partial I}{\partial y}V_y + \frac{\partial I}{\partial t}}{\sqrt{\left(\frac{\partial I}{\partial x}\right)^2 + \left(\frac{\partial I}{\partial y}\right)^2}} \tag{6}$$

where the magnitude of *D* is the distance between the global velocity point (V_x, V_y) and constraint line, and the miner sign means the force is moving the guessed global velocity point towards the constraint line. Based on the forcing function and a unit vector of correction force, the error can be represented by[5]

$$e = D * \frac{\nabla I}{|\nabla I|} = D * \left\langle \frac{\frac{\partial I}{\partial x}}{\sqrt{\left(\frac{\partial I}{\partial x}\right)^2 + \left(\frac{\partial I}{\partial y}\right)^2}}, \frac{\frac{\partial I}{\partial y}}{\sqrt{\left(\frac{\partial I}{\partial x}\right)^2 + \left(\frac{\partial I}{\partial y}\right)^2}} \right\rangle \tag{7}$$

Based on the error, each cell is supposed to produce a force *F* to move the global velocity proportional to the detected error *e*.

$$F = C \times e$$

where *C* is the confidence in local data, which can be calculated by using the equation shown below. This equation means a greater weight should be afforded to the correcting force in those higher contrast areas[5].

$$C = |\nabla I|^2 = \left(\frac{\partial I}{\partial x}\right)^2 + \left(\frac{\partial I}{\partial y}\right)^2 \tag{8}$$

Thus, the correction force can be represented by

$$F_x = -\left(\frac{\partial I}{\partial x}v_x + \frac{\partial I}{\partial y}v_y + \frac{\partial I}{\partial t}\right)\frac{\partial I}{\partial x} \tag{9}$$

$$F_y = -\left(\frac{\partial I}{\partial x}v_x + \frac{\partial I}{\partial y}v_y + \frac{\partial I}{\partial t}\right)\frac{\partial I}{\partial y} \tag{10}$$

F_x is the correction force in the x-axis component, and F_y is the correction force in the *y*-axis component. In other words, F_x is the error distance between V_x of the global velocity point and the point on the constraint line, and F_y is the error distance between V_y of the global velocity point and the point on the constraint line. The constraint-solving circuit or the cell is using operational circuits to achieve these two equations, and then uses these two forces to push the global velocity point onto the constraint line to obtain the real velocity of the motion or a unique solution of the Horn and Schunk equation, which can be represented by[5]

$$V_x = V_{globalx} + F_x = V_{globalx} - \left(\frac{\partial I}{\partial x}v_x + \frac{\partial I}{\partial y}v_y + \frac{\partial I}{\partial t}\right)\frac{\partial I}{\partial x} \tag{11}$$

$$V_y = V_{globaly} + F_y = V_{globaly} - \left(\frac{\partial I}{\partial x}v_x + \frac{\partial I}{\partial y}v_y + \frac{\partial I}{\partial t}\right)\frac{\partial I}{\partial y} \tag{12}$$

where the global velocity is set by the users, V_x is the real velocity in x-axis, and V_y is the real velocity in *y*-axis. In this project, photoreceptor which is consisting of phototransistors is used to receive light intensity and convert the light intensity into voltage signal, thus the light intensity in the correction force can be replaced by the voltage[5].

$$V_x = V_{globalx} + F_x = V_{globalx} - \left(\frac{\partial V}{\partial x}v_x + \frac{\partial V}{\partial y}v_y + \frac{\partial V}{\partial t}\right)\frac{\partial V}{\partial x} \tag{13}$$

$$V_y = V_{globaly} + F_y = V_{globaly} - \left(\frac{\partial V}{\partial x}v_x + \frac{\partial V}{\partial y}v_y + \frac{\partial V}{\partial t}\right)\frac{\partial V}{\partial y} \tag{14}$$

2. Materials and methods

2.1. Materials

All the materials required for this assignment and its type and quantities are shown in **Table 1**. The material list includes the software used in this project, circuit component in a cell, and the instruments used for measurement.

Table 1. Materials list.

Title	Type	Quantities
Multisim	Software for designing a cell	Don't care
Eagle	Software for designing layout	Don't care
Operational amplifier UA741cp (**Figure 4**)	Component in a cell	15
Multiplier AD633JN (**Figure 5**)	Component in a cell	12
Phototransistor TEPT4400 (**Figure 6**)	The input of cells	7
Resistors	Component in a cell	40
capacitors	Component in a cell	10
DC power supply	Supply DC voltage	1
Oscilloscope	Detect signal	1
Multimeter	Measure DC signal	1

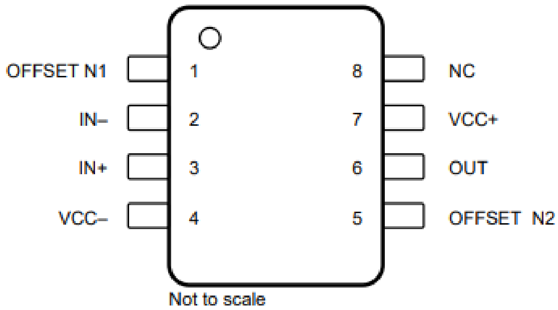

Figure 4. UA741CP.

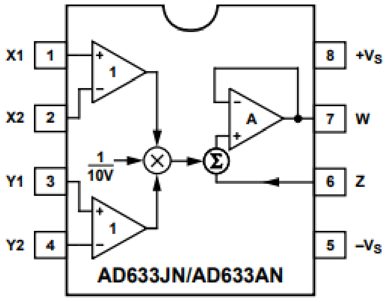

Figure 5. AD633JN.

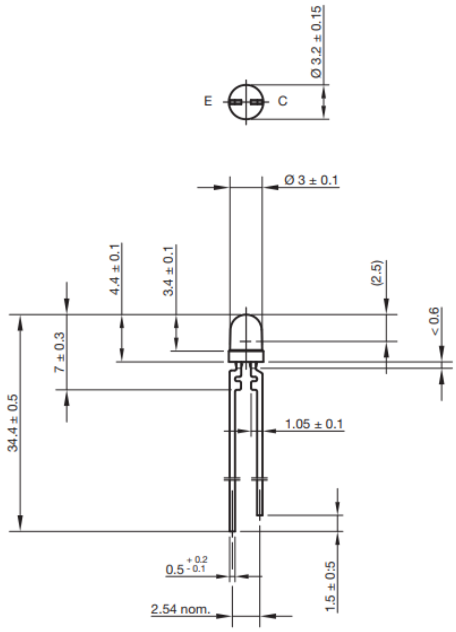

Figure 6. TEPT4400.

2.2. Methods

The project is broken into five steps, which include researching, simulating, building a cell on the breadboard and testing, presenting a cell on PCB and testing, printing more cells and connecting all the cells. In detail, for the first step, a book named "Analog VLSL and Neural System" is used to provide useful information in the project. Furthermore, the library of the University of Liverpool is also an effective website to search for information related to silicon retina. Moving to the next step, the software Multisim is used to build a cell and make a simulation according to the block diagram, which is shown in **Figure 7**. Following this, the operation amplifiers UA741CP and Multipliers AD633JN are used to build a cell on the breadboard to achieve the correction force Equations (9) and (10), and connecting three phototransistors to the cell and using an oscilloscope to test the performance of the built constraint-solving circuit (detecting the output signal from the *x*-direction and *y*-direction. Next, use the software to design a layout of a cell before soldering a cell on a PCB board. Finally, printing more cells and connecting all the cells to make them communicate with each other to get a more accurate speed of motion. The whole process is shown in the flowchart (**Figure 8**). Moreover, the whole process is not in one direction. In other words, the project can move reverse to upgrade or correct mistakes continuously. For example, when testing the circuit, the output signal is distorted or fluctuating, in this case, the circuit should first be returned to check whether there is a problem with the connection of the circuit, and returning simulation to check whether there is an environmental element. If the problem cannot be understood, books and the internet should be used to solve the problem.

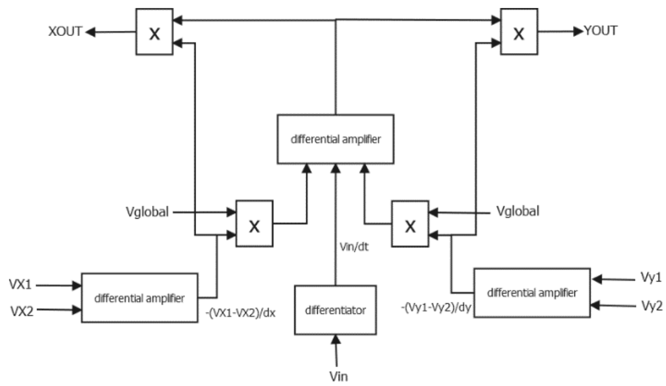

Figure 7. The block diagram of a constraint-solving circuit or a cell.

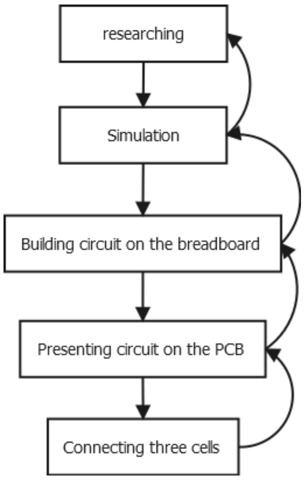

Figure 8. The flowchart of the whole process of this project.

3. Results

3.1. Building a cell in the Multisim

Because a cell is consisting of four multipliers, two differential amplifiers, one summing amplifier, and one differentiator, thus the first step is to build each component separately, and testing it individually.

Differential amplifier:

Figure 9 shows the differential amplifier built in Multisim.

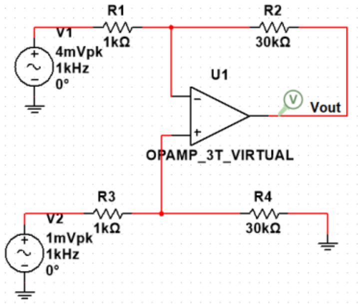

Figure 9. The schematic circuit of differential amplifier.

Figure 10 shows the transient simulation of the differential amplifier. The input $V1$ is 1 kHz, 4 mV sinewave, and the input $V2$ is 1 kHz, 1 m sinewave. The transfer function of the differential amplifier is

$$V_{out} = -\frac{R2}{R1}(V1 - V2) = -30 * (4 - 1)m = -90m \tag{15}$$

Thus, the amplitude output signal is supposed to be 1 kHz, 90 mV cosine wave, which is shown in **Figure 10**.

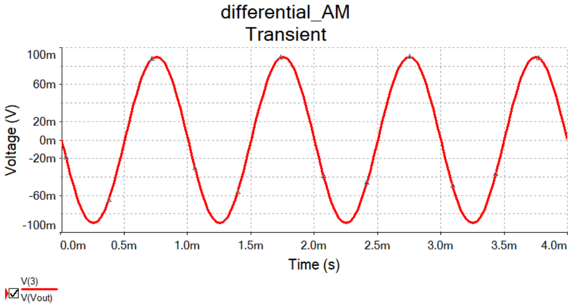

Figure 10. The transient simulation of the differential amplifier.

Summing amplifier:

Figure 11 shows the summing amplifier built in Multisim.

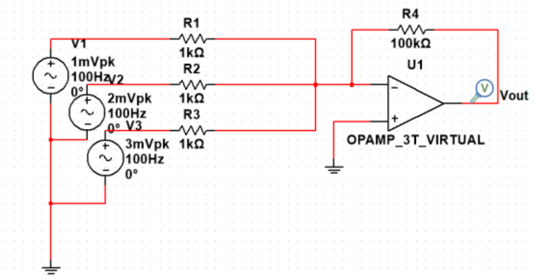

Figure 11. The schematic circuit of summing amplifier.

Figure 12 shows the transient simulation of the summing amplifier. The input *V*1 is 100 Hz, 1 mV sinewave, the input *V*2 is 100 Hz, 2 m sinewave, and the input *V*3 is 100 Hz, 3 m sinewave The transfer function of the summing amplifier is

$$V_{out} = -(\frac{R4}{R1}V1 + \frac{R4}{R2}V2 + \frac{R4}{R3}V3) \quad (16)$$

Thus, the gain of the summing amplifier can be calculated by

$$Av = -\frac{R4}{R1} = -100 \quad (17)$$

Thus, the amplitude output signal is supposed to be 100 Hz, 600 mV cosine wave, which is shown in **Figure 12**.

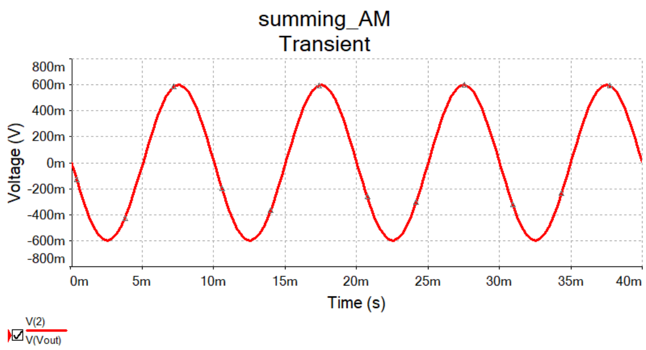

Figure 12. The transient simulation of the summing amplifier.

Differentiator:

Figure 13 shows the differentiator built in Multisim.

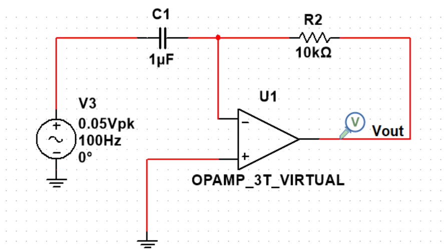

Figure 13. The schematic circuit of differentiator.

Figure 14 shows the transient simulation of the differentiator. The input *V*3 is 100 Hz, 0.05 V sinewave. The transfer function of the differential amplifier is

$$V_{out} = -RC\frac{dV3}{dt} \tag{18}$$

Thus,

$$V_{out} = -10k * 1u * \frac{d(0.05 * sin(200\pi t))}{dt} = -0.1\pi\cos(200\pi t) \tag{19}$$

Thus, the amplitude output signal is supposed to be 100 Hz, 0.1 πV sinewave, which is shown in **Figure 14**.

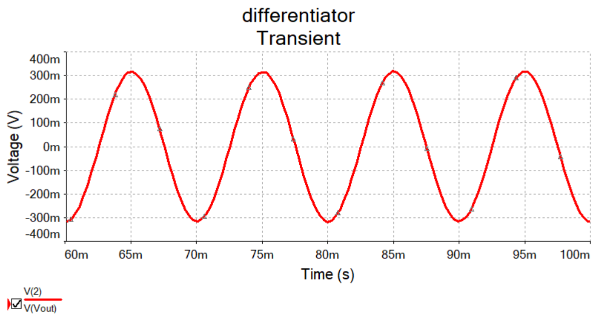

Figure 14. The transient simulation of the differential amplifier.

According to the bode plot, which is shown in **Figure 15**. The gain of the differentiator is linear with the frequency of the input signal. This is because the transfer function of differentiator includes the dV/dt. The phase change is about −90 degrees. This is because the sinewave becomes a miner cosine wave through the differentiator.

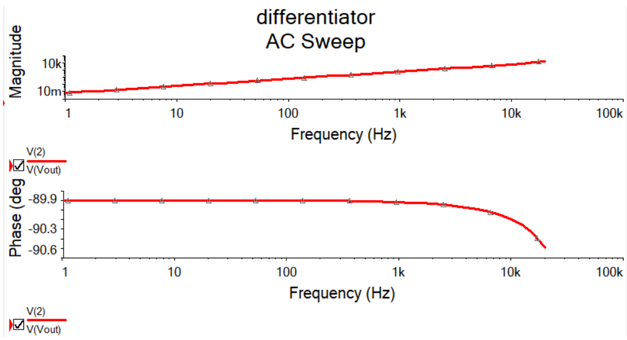

Figure 15. The bode plot of the differentiator.

Cell:

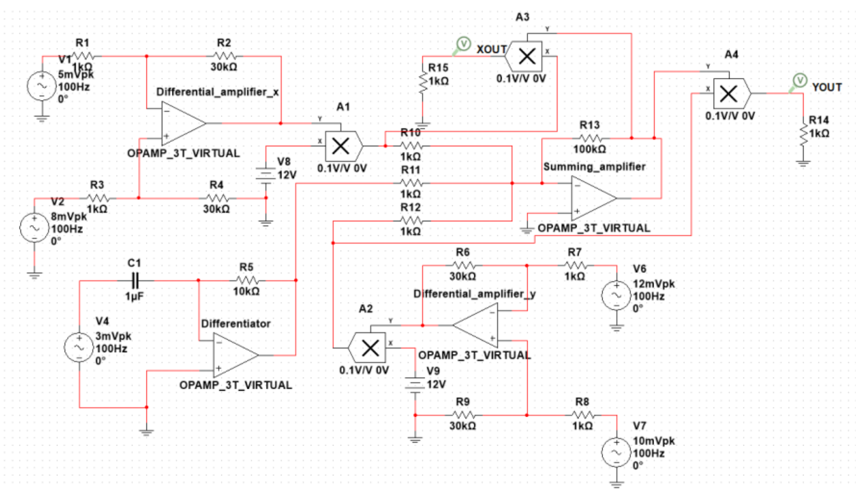

Figure 16. The schematic circuit of a cell.

Figure 16 shows the schematic circuit of a cell. The cell uses differential amplifier to achieve d*v*/d*x*, uses summing amplifier to achieve plus, uses multiplier to achieve multiplication, and uses differentiator to achieve dv/dt, thus the correction equation related to the voltage can be represented by the cell. In the cell, a global velocity is set to 12 V. The output of the *x*-axis XOUT indicates the error between the real velocity and the global velocity in *x* coordinate. The output of the *y*-axis YOUT indicates the error between the real velocity and the global velocity in y coordinate. In other words, the real velocity can be represented by

$$V_x = XOUT + V_{global} \tag{20}$$

$$V_y = YOUT + V_{global} \tag{21}$$

According to **Figure 16**, the gain of the differential-amplifier-*x* is 30, therefore, the output is

$$V_{diff-x} = -30(V1 - V2) = -30 * (5m - 8m)\sin(200\pi t) = 90\sin(200\pi t)\, mV \tag{22}$$

The gain of the differential-amplifier-*y* is 30, therefore, the output is

$$V_{diff-y} = -30(V6 - V7) = -30 * (12m - 10m)\sin(200\pi t) = -60\sin(200\pi t)\, mV \tag{23}$$

The transfer function of the differentiator is

$$V_{diffr} = -10k * 1u * \frac{d(3m * sin(200\pi t))}{dt} = -6\pi\cos(200\pi t)\, mV \tag{24}$$

The gain of the multiplier A1 is 0.1, thus the output is

$$V_{A1} = 0.1 * 12 * 90\sin(200\pi t)\, m = 108\sin(200\pi t)\, mV \tag{25}$$

The gain of the multiplier A2 is also 0.1, thus the output is

$$V_{A2} = 0.1 * 12 * -60\sin(200\pi t)\, m = -72\sin(200\pi t)\, mV \tag{26}$$

The gain of the summing amplifier is 100, thus the output is

$$V_{sum} = -100 * \left(V_{diffr} + V_{A1} + V_{A2}\right) = -3.6\sin(200\pi t) + 1.9\cos(200\pi t)\, V \tag{27}$$

The maximum voltage is approximately 4 V, and the minimum voltage is −4 V. The gain of multiplier A3 is 0.1, thus the output is

$$XOUT = V_{sum} * V_{diff-x} * 0.1 = -32.4\sin(200\pi t)^2 + 17.1\sin(200\pi t)\cos(200\pi t)\, mV \tag{28}$$

The gain of multiplier A4 is 0.1, thus the output is

$$YOUT = 0.1 * V_{sum} * V_{diff-y} = 21.6\sin(200\pi t)^2 - 11.4\sin(200\pi t)\cos(200\pi t)\, mV \tag{29}$$

Figure 17 shows the transient simulation of the cell. The red line indicates the output from the *x*-axis, and the blue line indicate the output from *y*-axis. The simulation is basically following the deduced Equations (27) and (28). According to Equation (27), the amplitude of XOUT should be negative sinewave (the minimum voltage is about 50 mV, the maximum voltage is about 0 V), and the frequency should be 200 Hz because the frequency of output signal should be becoming twice after the multiplication of two sinewaves. According to Equation (28), the amplitude of YOUT should be positive sinewave (the minimum of voltage is about 0 V, the maximum voltage is about 30 mV), and the frequency should be 200 Hz because the frequency of output signal should be becoming twice after the multiplication of two sinewaves.

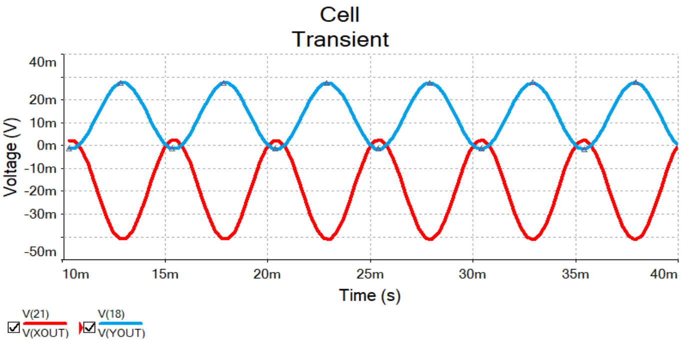

Figure 17. The transient simulation of the cell.

3.2. Building a cell on the breadboard

Figure 18 shows a cell built on the breadboard. In reality, there are noises in the output, and to reduce the noise to improve the quality of output signal, two low pass filters, which are consisting of capacitors and resistors in series.

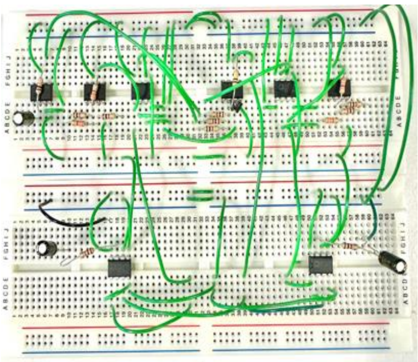

Figure 18. A cell built on the breadboard.

Using sinewaves to test:

When the inputs are the same as the simulation in Multisim, the outputs are also basically the same as the results in the simulation. XOUT is negative sinewave, and YOUT is positive sinewave. To make it easy to read, the button is used to put the output signal to the centre. To be more specific, the amplitude of XOUT should be sinewave (the amplitude of the output signal is about 20 mV), and the frequency should be 200 Hz because the frequency of the output signal should be become twice after the multiplication of two sinewaves, which is shown in **Figure 19**. The amplitude of YOUT should be sinewave (the amplitude of the output signal is about 15 mV, which is less than the amplitude of XOUT), and the frequency should be 200 Hz because the frequency of output signal should be becoming twice after the multiplication of two sinewaves, which is shown in **Figure 20**.

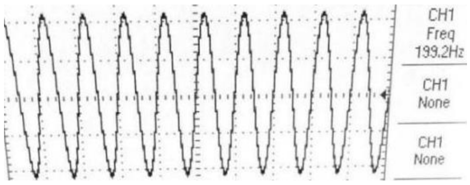

Figure 19. The output of XOUT when using sinewaves.

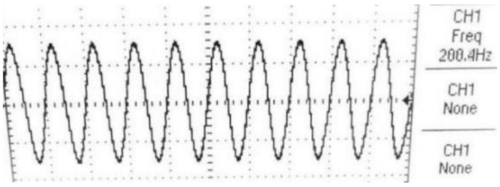

Figure 20. The output of YOUT when using sinewaves.

Using phototransistors to test:

A photoreceptor, which is only consisting of phototransistors, is used to receive the light intensity and to convert the light intensity signal into a voltage signal. To reduce the number of used phototransistors, the distribution of the phototransistors on the photoreceptor is similar to the distribution of the atom in silicon. In other words, the phototransistors on the photoreceptor can be shared, which is shown in **Figure 21**. Two phototransistors on the horizontal are detecting the motion on the x-axis, and two phototransistors on the vertical are detecting the motion on the *y*-axis. Furthermore, the yellow one is the shared phototransistor in the *x*-axis and *y*-axis.

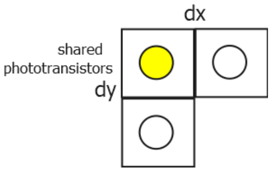

Figure 21. The distribution of phototransistor on a photoreceptor.

When the object is moving as **Figure 22** shows, the velocity in *x*-axis is larger than in *y*-axis, which means the cell need large correction force in *x*-axis, thus the output XOUT is different with the output YOUT, and the amplitude of the XOUT is larger than the YOUT.

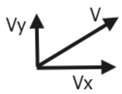

Figure 22. The motion when testing a cell on the breadboard.

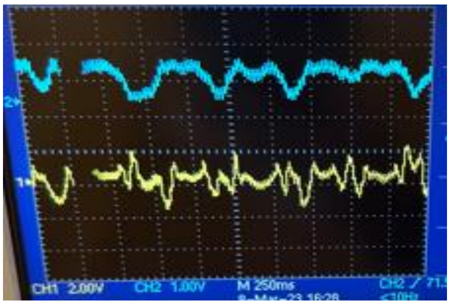

Figure 23. The outputs from XOUT and YOUT when testing a cell on the breadboard.

3.3. Presenting a cell on the PCB

Layout design:

Figure 24 shows the layout designed in Eagle. The PCB has two layers, which are the top layer and the bottom layer. The bule lines are wires on the bottom layer, and the red lines are wires on the top layer. Junctions are used to make a connection between top and bottom layers.

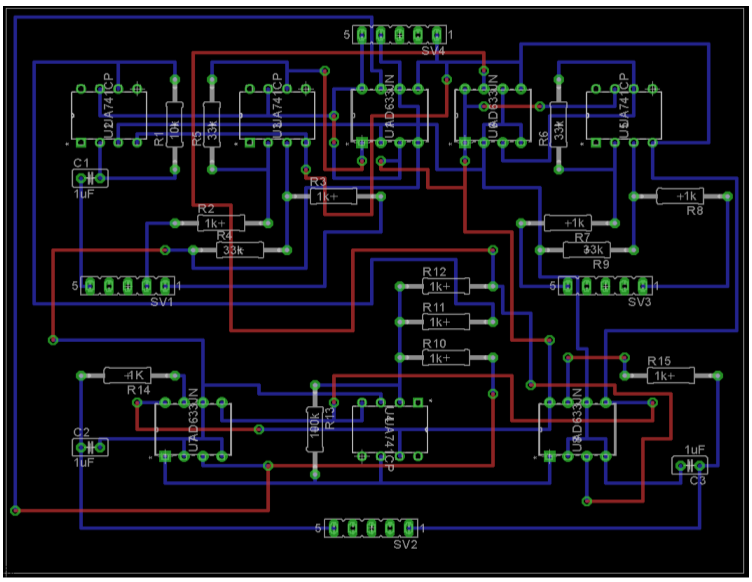

Figure 24. The layout designed in Eagle.

Soldering:

Figure 25 shows the cell soldered on the PCB board.

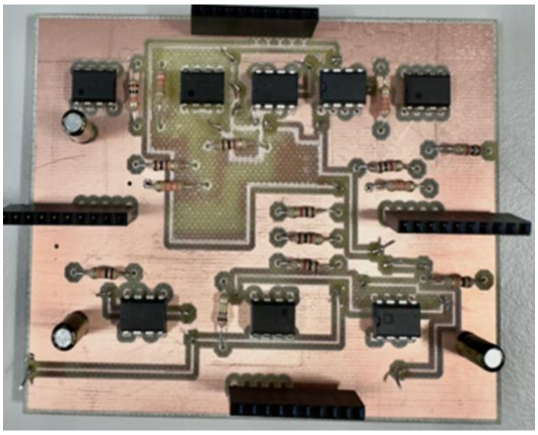

Figure 25. The cell soldered on the PCB board.

Connecting the photoreceptor to test:

When the object is moving fast (40 cm/s), the frequency of the output signals XOUT and YOUT will be larger. When the object is moving slow (20 cm/s), the frequency of the output signals XOUT and YOUT will be smaller. This is shown in **Figures 26** and **27** (The blue signal is XOUT and the yellow signal is YOUT).

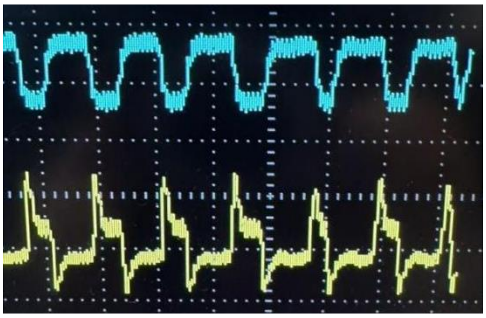

Figure 26. The output signal when the object is moving fast.

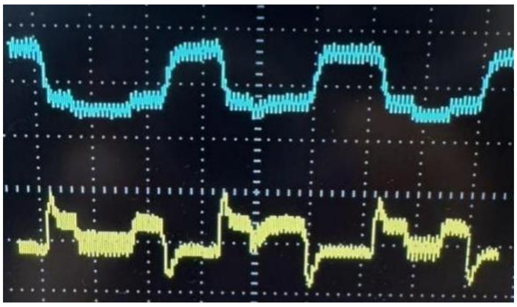

Figure 27. The output signal when the object is moving slow.

When the object is moving horizontally, because in reality the horizontal motion cannot be fully achieved, this means that there is also an output in the *y*-direction but the amplitude of the output of the signal in the *x*-direction is greater than in the *y*-direction. When the object is moving vertically, because in reality the vertical motion cannot be fully achieved, this means that there is also an output in the *x*-direction but the amplitude of the output of the signal in the y-direction is greater than in the *x*-direction. This is shown in **Figures 28** and **29** (The blue signal is XOUT and the yellow signal is YOUT).

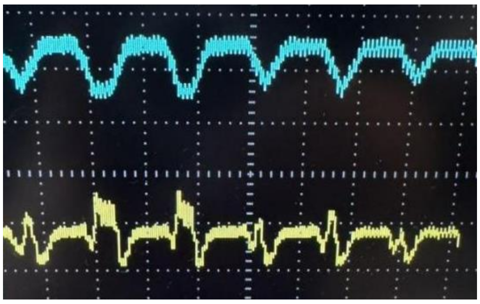

Figure 28. The output signal when the object is moving horizontally.

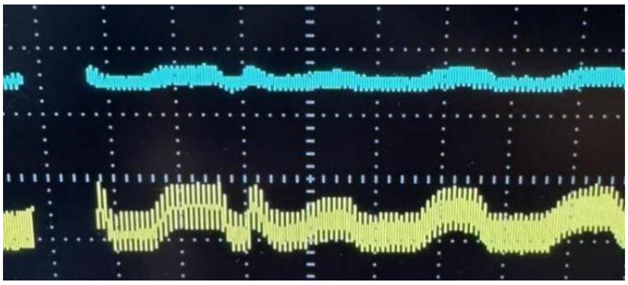

Figure 29. The output signal when the object is moving vertically.

When the object is moving upward at 45 angle or is moving downward at 45 angle, the outputs from the cell should be different in these two conditions. Because the different directions of motion result in different velocity magnitudes in the *x* and *y* directions, the output signals have different amplitudes.

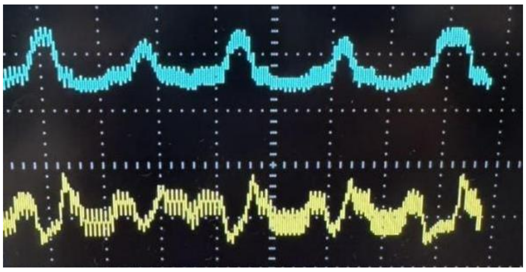

Figure 30. The output signal when the object is moving upward at an angle.

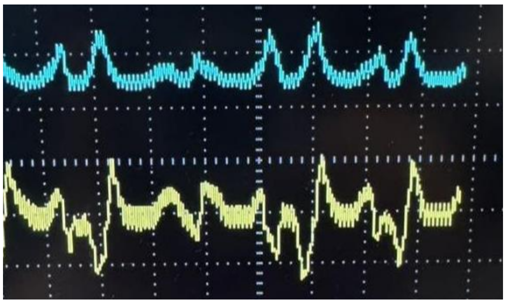

Figure 31. The output signal when the object is moving downward at an angle.

3.4. Connecting three cells altogether

Adding more phototransistors on the photoreceptor:

As mentioned above, two horizontal phototransistors are detecting the motion in x-axis, and two vertical phototransistors are detecting the motion in y-axis. If there are three cells, three phototransistors are needed, which are distribute as **Figure 32** shows. The yellow circles are shared phototransistors.

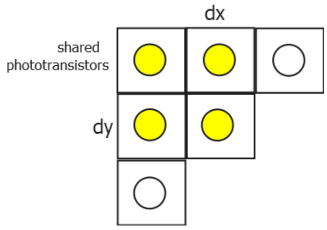

Figure 32. The distribution of phototransistor when connecting three cells.

Connecting three cells:

Using the layout design to print two more cells, and then connecting the output XOUT of three cells directly to make the system can detect the motion in x-axis more accurate (averaging the signal), and connecting the output YOUT of three cells directly to make the system can detect the motion in y-axis more accurate. This method can make three cells communicate with each other to get more accurate output, which is similar to the phase locked loop. When the object is moving fast (40 cm/s), the frequency of the output signals XOUT and YOUT will be larger. When the object is moving slow (20 cm/s), the frequency of the output signals XOUT and YOUT will be smaller. This is shown in **Figures 33** and **34** (The yellow signal is XOUT and the blue signal is YOUT). Compared with the outputs from one cell, the output signals become clearer, this is because the noise will be reduced when three cells are communicating each other. Furthermore, the system become more sensitive. This is because more phototransistors are used to detect motion.

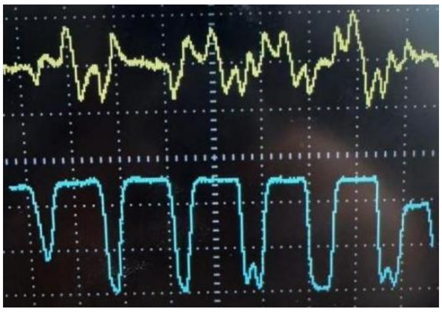

Figure 33. The output signal from three cells when the object is moving fast.

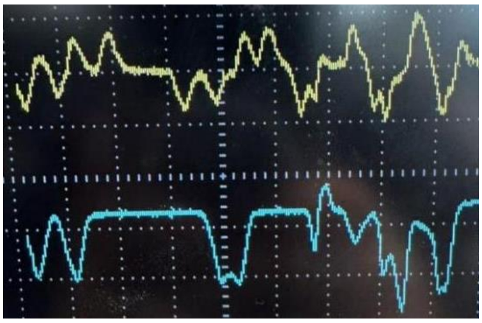

Figure 34. The output signal from three cells when the object is moving slow.

When the object is moving horizontally, because in reality the horizontal motion cannot be fully achieved, this means that there is also an output in the *y*-direction but the amplitude of the output of the signal in the *x*-direction is greater than in the y-direction. When the object is moving vertically, because in reality the vertical motion cannot be fully achieved, this means that there is also an output in the *x*-direction but the amplitude of the output of the signal in the *y*-direction is greater than in the *x*-direction. This is shown in **Figures 35** and **36** (The yellow signal is XOUT and the blue signal is YOUT). Compared with the outputs from one cell, the difference between XOUT and YOUT is large because using three cells improves the accuracy of the system.

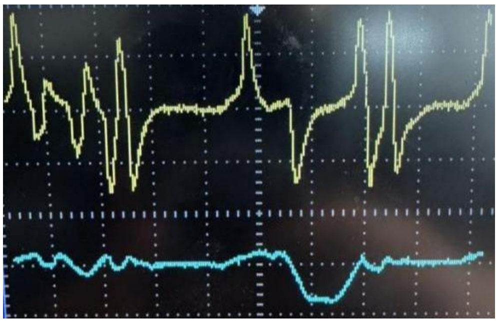

Figure 35. The output signals from the three cells when the object is moving horizontally.

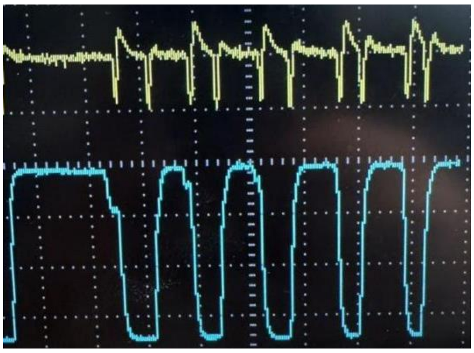

Figure 36. The output signals from the three cells when the object is moving vertically.

When the object is moving upward at a 30 angle or is moving downward at a 60 angle, the outputs from the cell should be different in these two conditions. Because the different directions of motion result in different velocity magnitudes in the *x* and *y* directions, the output signals have different amplitudes. Compared with the outputs from one cell, the output signals become clearer and the system becomes more sensitive. The difference is also becoming clearer between the two types of motions.

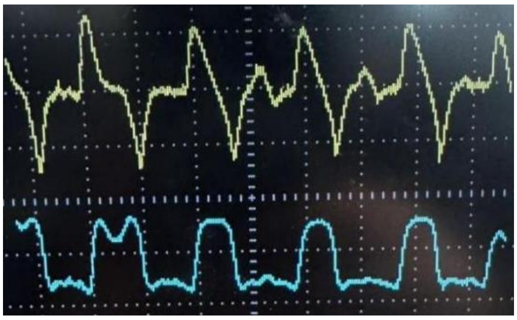

Figure 37. The output signals from the three cells when the object is moving upward at an angle.

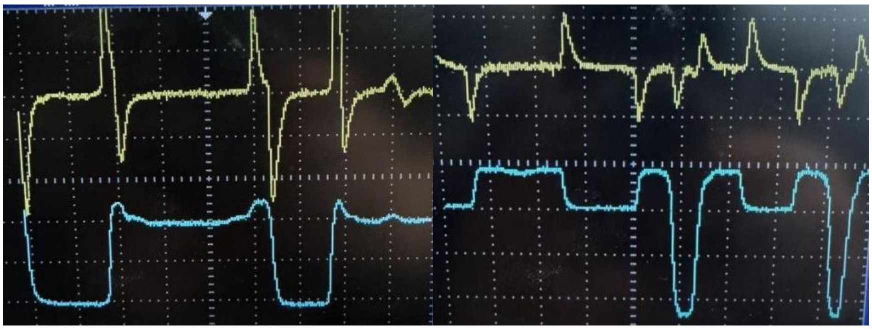

Figure 38. The output signals from the three cells when the object is moving downward at an angle.

4. Discussion

4.1. Errors analysis

Cannot strictly moving horizontally and vertically:

At first, in reality the horizontal and vertical motion cannot be strictly achieved, this means that there is also an output in the *x*-direction or *y*-direction, thus when analysing the outputs signal when moving horizontally or vertically, this condition should be considered.

Random error:

Moreover, in the environment, there are noises, which will influence the outputs of the cell. This can be solved by adding two pass filters in the cell. Each component is very closed with each other, which causes the interference. This can be solved by connecting more than one cells to make errors cancel each other to get more accurate speed. The error mentioned above is random error, which can be reduced by making an average.

Resistor tolerance:

Furthermore, all the resistors and capacitors used in this project has a tolerance. The right of all the resistors in the cell is gold, which means the tolerance of all the resistors in the cell is 5%. This will change the gain of each component in the cell and then change the outputs of the cell. For the differential amplifier, the gain of the differential amplifier is

$$G_{diff} = -\frac{R2(1 \pm 5\%)}{R1(1 \pm 5\%)} \tag{30}$$

Thus, the maximum error occurs when the sign before the error is opposite

$$G_{diff} = -\frac{R2(1 + 5\%)}{R1(1 - 5\%)} \approx -\frac{R2}{R1}(1 + 10\%) = 33 \tag{31}$$

For the summing amplifier, the gain of the summing amplifier is

$$G_{sum} = -\frac{R4(1 \pm 5\%)}{R1(1 \pm 5\%)} \tag{32}$$

Thus, the maximum error occurs when the sign before the error is opposite.

$$G_{diff} = -\frac{R4(1 + 5\%)}{R1(1 - 5\%)} \approx -\frac{R4}{R1}(1 + 10\%) = 110 \tag{33}$$

For the Differentiator, the gain of the differentiator is

$$V_{out} = -RC\frac{dVin}{dt} \tag{34}$$

Thus, the maximum error occurs when tolerance is +5%.

$$G_{diffr} = -R(1 + 5\%)C\frac{dVin}{dt} \tag{35}$$

Finite open loop gain:

In the analysis, the gain of the operational amplifiers is assumed to be positive infinite, but in reality, the gain of the operational amplifiers UA741CP has finite open loop gain. This will cause the error in the gain. The real gain is given by

$$A = \frac{1}{\beta}\left(\frac{1}{\frac{1}{\alpha\beta} + 1}\right) = A_{ideal} * (\frac{T}{T + 1}) \tag{36}$$

where α is the open loop gain of the amplifier, β is the feedback of the amplifier, and T is $\alpha\beta$. Therefore, the gain error can be defined as:

$$E = \frac{A\text{âˆ’}A_{ideal}}{A_{ideal}} = \text{âˆ’}(\frac{1}{T+1}) \tag{37)(37}$$

Because, in reality *T* is much larger than 1, thus, the error equation can be simplified.

$$E = -\frac{1}{T} \tag{38}$$

For the UA741CP, according to the datasheet, the open loop gain of UA741CP is 106 dB, which is approximately 20,000. The feedback of differential amplifier is 1/30, the feedback of summing amplifier is 1/100, and the feedback of the differentiator is 1/100, thus the gain error of differential amplifier and summing amplifier can be calculated:

$$Ediff = -\frac{1}{T} = -\frac{1}{20000 * \frac{1}{30}} = -1.5 * 10^{-3} \tag{39}$$

$$Esum = -\frac{1}{T} = -\frac{1}{20000 * \frac{1}{100}} = -5 * 10^{-3} \tag{40}$$

$$Ediffr = -\frac{1}{T} = -\frac{1}{20000 * \frac{1}{100}} = -5 * 10^{-3} \tag{41}$$

Finite bandwidth:

In the analysis, the bandwidth of the operational amplifiers is assumed to be positive infinite, but in reality, the bandwidth of the operational amplifiers UA741CP has finite bandwidth. This will cause the error in the gain. The real gain is given by

$$A = A_{ideal} * A(\omega) = A_{ideal} * (1 - \varepsilon) \tag{42}$$

where $A(w)$ can be calculated by Equation (42), and ε can be calculated by Equation (43).

$$A(w) = \frac{1}{1 + \frac{j\omega}{\omega_0}} \tag{43}$$

where ω_0 is the corner frequency, which is defined as the frequency at which the gain is reduced by 3 dB.

$$\varepsilon = 1 - A(\omega) \rightarrow |\varepsilon| = \sqrt{\frac{\omega^2}{\omega^2 + \omega_0^2}} \tag{44}$$

For the UA741CP, according to the datasheet, the bandwidth of UA741CP is 1 MHz, and the input frequency is small and varied from 1 Hz to 30 Hz, thus ε can be simplified.

$$|\varepsilon| = \sqrt{\frac{\omega^2}{\omega^2 + \omega_0^2}} \approx \frac{\omega}{\omega_0} \tag{45}$$

Thus, the gain error of differential amplifier, summing amplifier, and differentiator is

$$E = A_{ideal} * |\varepsilon| = \frac{30}{1\,M} * A_{ideal} = 3 * 10^{-5} * A_{ideal} \tag{46}$$

Finite input resistance and nonzero output resistance:

In the analysis, the operational amplifiers are assumed to be ideal voltage amplifiers, which means the input resistance is assumed to be infinite and the output resistance is assumed to be 0, but in reality, the operational amplifiers UA741CP has finite input resistance and nonzero output resistance. This will cause the error in the gain. The real gain is given by

$$Ar = \frac{V_0}{Vs} = \frac{A_{ideal} * Vin}{Vin/(\frac{r_{in}}{Rs + r_{in}})} = A\frac{r_{in}}{Rs + r_{in}} \tag{47}$$

where Vin is input signal, r_{in} is the input resistance, and Rs is the source resistance. For the UA741CP, according to the datasheet, the input resistance of UA741CP is 2 MΩ, and the source resistance of the differential amplifier is 1 kΩ, and the source resistance of the summing amplifier is 333 Ω, because the input resistance is much larger than the source resistance, thus the equation of 47 can be simplified.

$$Ar = A(1 - \frac{Rs}{r_{in}}) \tag{48}$$

Thus, the gain error of differential amplifier, and summing amplifier, are

$$Ediff = A * \frac{Rs}{r_{in}} = A_{ideal} * \frac{1000}{1M} = 10^{-3} A_{ideal} \tag{49}$$

$$Esum = A * \frac{Rs}{r_{in}} = A_{ideal} * \frac{333}{1M} = 3.33 * 10^{-4} A_{ideal} \tag{50}$$

Multiplier:

Finally, for the multiplier AD633JN, the multiplier errors mainly include input and output offsets, the scale factor errors, and the nonlinearity of the multiplication core. For the input and output offsets, it will cause the gain error. Foran irreducible nonlinear component. the nonlinearity of X and Y are typically 0.4% and 0.1% of full scale, respectively. Scale factor error is typically 0.25% of full scale. High impedance Z input should always be referenced to the ground point of the system being driven, especially if it is remote. Similarly, the differential X and Y inputs should be referenced to their respective grounds in order to achieve the full accuracy of the AD633.

4.2. Limitations analysis

The area of the photoreceptor:

The first limitation is the accuracy of the output signal is influenced by the area of the photoreceptor. To be more specific, the output voltage on the global velocity on the lines is determined by the total charge on the node, which can be calculated by

$$M \propto \int i_{tot} dt \tag{51}$$

The total current can be calculated by using the output current miners the current through the load resistance.

$$i_{tot} = i_{out} - i_L \tag{52}$$

If the system is in steady state, the total charge on the node is 0, thus,

$$i_{out} = i_L = M \frac{1}{RL} \tag{53}$$

where M is the output voltage on the global velocity, and RL is the load resistance.

The output current from x-axis is produced by the multiplier, which can be represented by

$$i_{out} = M \frac{1}{RL} = -\left(M \frac{\partial I}{\partial x} + \frac{\partial I}{\partial t}\right) \frac{\partial I}{\partial x} \tag{54}$$

where I is light intensity. Solving M, an equation can be obtained:

$$M = -\frac{\frac{\partial I}{\partial x}}{(\frac{\partial I}{\partial x})^2 + \frac{1}{RL}} \frac{\partial I}{\partial t} \tag{55}$$

When $(\frac{\partial I}{\partial x})^2$ is much greater than $1/RL$, the equation can be represented by

$$M = -\frac{\partial I / \partial t}{\partial I / \partial x} \tag{56}$$

When $(\frac{\partial I}{\partial x})^2$ is approaching zero, which means it becomes much smaller than $1/RL$, the equation can be simplified by

$$M = -\frac{\partial I}{\partial x} * \frac{\partial I}{\partial t} * RL \tag{57}$$

According to Equations (55) and (56), as contrast in the image is reduced (the area of the photoreceptor is decreasing), the motion output change smoothly to become a function linear with dI/dx and dI/dt, and as contrast in the image is continuously increasing (the area of the photoreceptor is increasing), the output will approximate a hyperbolic response, which is shown in **Figure 39**. However, for a very small dI/dx, which means the view of the field is too small, the system will fail to output the accurate velocity, thus in this project, the area of photoreceptor should be big enough to ensure the output velocity is accurate. The distance between each phototransistor in the photoreceptor should not be smaller than 3 cm.

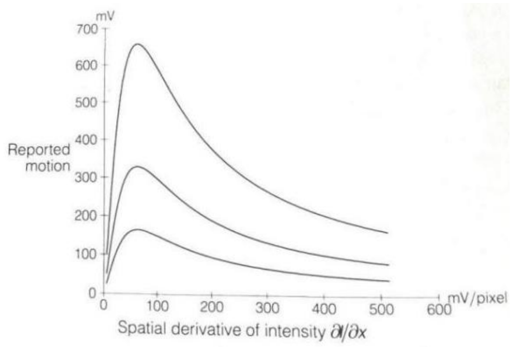

Figure 39. Motion-response curve as a function of dI/dx of at different frequency[5].

Light intensity:

Figure 40 shows the phototransistor circuit. The light intensity will change the base voltage, thus changing the output voltage. There are many phototransistors in a photoreceptor, this results in different phototransistors easily being under different light intensities, and the different light intensities will make the DC offset in their output signals differently, and when their outputs are connected to a cell, the outputs will be subtracted in the differential amplifier, although the difference in DC offset is very small, the differential amplifier and the summing amplifier whose gain is supposed to be large enough to amplify the small signal from the phototransistor will result in a large DC offset value in the output signal. The solution is adding a low pass filter to filter the DC voltage in the output signal.

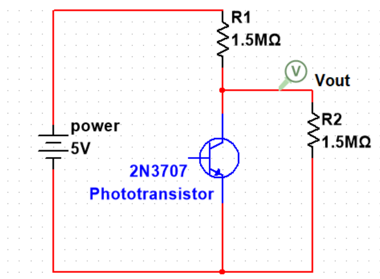

Figure 40. The phototransistor circuit.

DC offset:

According to **Figure 40**, 1.5 MΩ resistors are used to build the phototransistor circuit. As mentioned in error analysis, the resistors used in this project has 5% tolerance. This will cause different phototransistor circuit has different potential divider in the photoreceptor and the different light intensities will make the DC offset in their output signals different, and when their outputs are connected to a cell, the outputs will be subtracted in the differential amplifier, although the difference in DC offset is very small, the large gain of the differential amplifier and the summing amplifier will result in a large DC offset value in the output signal. The solution is adding a low pass filter to filter the DC voltage in the output signal.

Slew rate and amplification range:

The definition of slew rate is the fastest rate at which the output voltage of a closed-loop amplifier can change[6]. It is expressed in V/us. This value shows the maximum rate of change that the output can provide when the op-amp is operating normally. When the output signal wants to achieve a faster change than this rate, the op-amp cannot provide it, resulting in a distorted output waveform. In other words, when the amplitude or frequency of the input signal is too large, the output cannot follow the change in the input signal due to the rise time and fall time, thus becoming distorted. For example, in this project, when using sinewave to test the cell on the breadboard, if the amplitude or frequency of input sinewaves are too large, the output signals will become triangle waves, not sinewaves, which is shown in **Figure 41**. According to the datasheet, the operational amplifier UA741CP has 0.5 V/us slew rate. Moreover, in this project, the supply voltage of the operational amplifiers is 12 V, which means the maximum amplitude of the output signal cannot exceed 12 V.

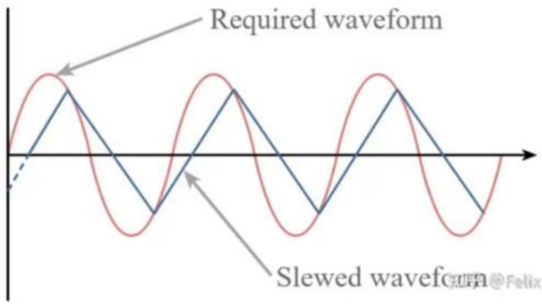

Figure 41. The slewed waveform[6].

4.3. Literature review

4.3.1. 1 kHz 2D visual motion sensor

The chip photo in **Figure 42** shows the architecture of the MDC2D retinal chip. The chip has a 20 × 20 pixel array and scanner circuitry that allows the transfer of local pixel information off-chip[7]. By using the optimized I2A algorithm, the global motion stream can be calculated at sampling rates up to 1 kHz. The SNR for natural scenes is 10 and the minimum contrast for saturated motion signals is 0.3. The current sensor weighs 11 g (6 g without lens) and measures 2.56. It consumes about 170 mW of total power from a 5 V USB supply (6 mW for the sensor, 164 mW for the dsPIC), and the dsPIC controller occupies 12% of the available clock cycles at a sampling rate of 1 kHz[7]. The measurements in contrast sensitivity and outdoor cloud scene suggest that consideration of image statistics will be a necessary enhancement in the future, as motion signals clearly depend on adequate image contrast. The low optical velocity measurements may be due to low image contrast rather than low velocity. Such a contrast metric has been computed, which reports the sum of squared spatial gradients in the and directions, but they are not currently available as outputs. These statistics can in principle be used to measure the confidence level of the velocity and speed measurements[7]. The use of high frame rates comes at the cost of reduced sensitivity to slow motion. Therefore, in a more refined implementation, a form of automatic sample rate control would be needed that could be based on feedback control of the scalar-derived quantities[7]. Specifically, the quantity and the sum product of the measured time and space derivatives. Unlike the case of conventional image sensors, the frame rate control only needs to control the sensitivity to motion, not the pixel exposure time, which is automatically set by the photoreceptor circuitry in each pixel[7].

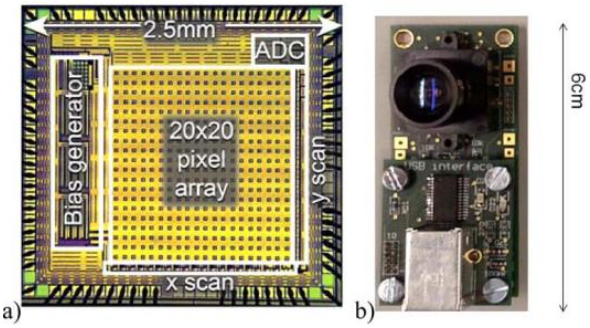

Figure 42. IC die photo and PCB implementation. **(a)** die photo of MDC2D 2D vision sensor; **(b)** miniaturized circuit board. The dsPIC controller is on the back of the PCB. The USB interface is a daughterboard that can be removed for embedded operation[7].

4.3.2. Bio-inspired stereo vision system with silicon retina imagers

A silicon retinal imager can be used in stereo vision system because cameras derived from the human visual system have the advantage of high temporal resolution of up to 1 ms and a dynamic range of ~120 dB for processing in various lighting conditions[8]. The silicon retina transmits asynchronous data called address events (AE). Different stereo matching algorithms can be used, but they are usually applicable to full-frame images. The AE data from silicon retina sensors must fit into full-frame region-based and feature-based stereo matching algorithms. **Table 2** shows the data rate of the existing silicon retina imager[8].

Table 2. The data rate of the existing silicon retina imager[8].

	128 × 128 silicon retina
Transfer data	50.000^{b} AE/s
Data size	64^{d} bit/AE
Transfer rate	~3.2 MBit/s

4.3.3. Artificial silicon retina for patients with retinitis pigmentosa

Firstly, the neurotrophic salvage effect on visual function reported in the human pilot study of RP patients implanted with ASR devices persisted during up to 8 years of follow-up, and a similar neurotrophic effect was confirmed in patients with additional implanted RP. Although the maximum improvement in visual acuity declined in many patients during the follow-up period, all patients still had improved visual acuity at the most recent follow-up examination compared to the preoperative period. The mechanism of the neurotrophic effect may involve upregulation of the expression of growth factors such as Fgf2 through electrical stimulation[9]. Secondly, the use of a modified version of the CGAT (GAT) and CHS/CLS CCT allows for more reliable measurements of visual acuity and color vision in patients with ASR implants and other forms of vision loss at a lower range, and the potential usefulness of these tests for future clinical studies evaluating the treatment of patients with severe vision loss[9]. Thirdly, the ASR in the eyes of re-sighted patients is tolerable during follow-up of up to approximately 8 years and has a functional life of approximately 20 years based on analysis of the external implants. Subretinal implanted ASR devices should be evaluated as a treatment for RP in larger prospective studies and should be considered for preliminary studies in other retinal degenerative diseases, such as dry AMD[9].

4.3.4. A programmable silicon retina with pattern recognition

The operation of the circuit is based on the classification (or programming) of retinal pixels as black or white pixels, and the determination of the total current generated by all pixels of the same type when projecting the image on the circuit[10]. The measurement of these two currents (called black and white pixel currents) and their comparison with the expected values can determine whether the projected image resembles the reference image used to program the pixels. Programming the pixels as white or black pixels is achieved by first projecting the reference image onto the retina. The current generated by each pixel is then compared to a threshold value. If that current is greater than the threshold, the pixel is considered a white pixel, otherwise it is considered a black pixel. In addition, to verify that the circuit can be implemented in standard CMOS technology[10], a prototype non-programmable test retina has been fabricated and characterized in 1.2 μm technology. The results show that the CMOS process is suitable for fabricating the circuit. The values and variations of the currents were large enough to be measured, and the response time of the circuit was found to be on the order of 100 ns. This time is very short, so the output signal is almost instantaneous, allowing for real-time application of the circuit[10].

4.3.5. Event-based camera

Event-based cameras, which is consisting of the silicon retina, are very promising sensors for high-speed mobile robots, self-driving cars and drones, and many other applications ranging from next-generation IoT to low-latency access to visual medical information. The data rate output by event-based vision sensors depends on the scene type and the speed of motion. Moreover, the camera uses a bandwidth prediction model by considering scene content and motion speed[11]. According to this study, the neuromorphic event rate varies exponentially with scene complexity, and the average gradient approximation based on Sobel and Prewitt shows the best-fitting goodness of fit. In addition, the relationship between sensor velocity and event rate is investigated, and found it to be linear. Based on these analyses, a two-parameter exponential model is proposed for the dependence of event rate on scene complexity and sensor velocity[11]. According to the results, the model based on Sobel and Prewitt shows a prediction accuracy of about 88.4% for the outdoor dataset and an overall prediction performance of about 84%[11]. The Prediction accuracy of the Sobel-based mean gradient model on different outdoor and indoor datasets are shown in **Figure 43**[11].

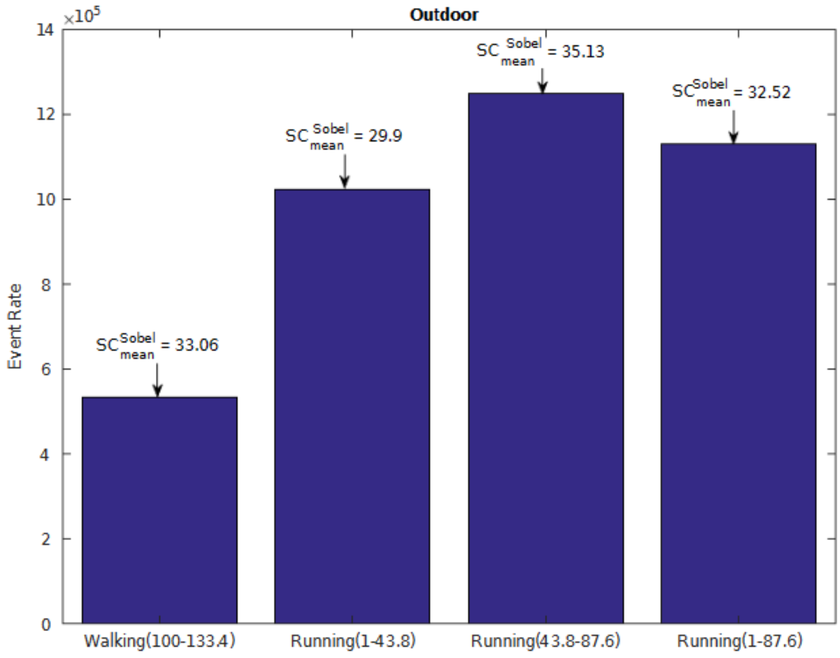

Figure 43. Event rate plot of the extracted sequences from the outdoor data. The text arrows report themean gradient of the extracted sequences[11].

According to the above nearly 20 years of literature, people's exploration of the silicon retina is more and more extensive, more and more in-depth, the development of the silicon retina has reached a very mature stage, specifically, the definition of the silicon, the output results and analysis of the circuit of the silicon retina can be found in the literature, which means that the project will have reliable literature support, which makes the project have sufficient knowledge to complete. But objectively speaking, the application of the silicon retina in the literature is very limited, which shows that the application of the automobile is not very extensive, nor is it widely accepted.

4.4. Industrial relevance

4.4.1. Medical area

The silicon retina can be applied to a medical area. To be more specific, according to the research, approximately 7 million people who live in developed countries are diagnosed with age-related eye diseases and a large number of people worldwide suffer from diseases related to the retina[12]. The silicon retina that mimics the neural circuitry of a real retina provides better bionic eyes for those with vision loss to walk and work. Furthermore, a pilot study has been done to evaluate the reliability of the silicon retina[9]. In this research, a light-activated micro photodiode array chip, known as an artificial silicon retina (ASR shown in **Figure 43**), was implanted under the retinas of six patients with retinitis pigmentosa (RP) for a period of 18 months. The ASR induced retinal neurotropism under the effect of electricity to save visual acuity, contrast, and colour perception. Under the observation, the ASR is tolerated and function over a longer period of time to slow the appearance of the vision loss[9], and the neurotrophic effects develop and persist in the additional implanted RP patients. Furthermore, over the years, a variety of wide dynamic range (WDR) CMOS image sensors have been proposed in an attempt to extend the operating luminosity range into the visible spectrum while maintaining sensitivity to small changes in the average luminosity of each operating range[12]. Although WDR image sensors capture images with a luminance range of up to 7 decimal degrees, they provide different contrast sensitivity at different average luminance levels. Event-based vision applications and medical applications typically require high and constant sensitivity over a large photometric range to detect small temporal and/or spatial variations in intensity under multiple illumination conditions[13].

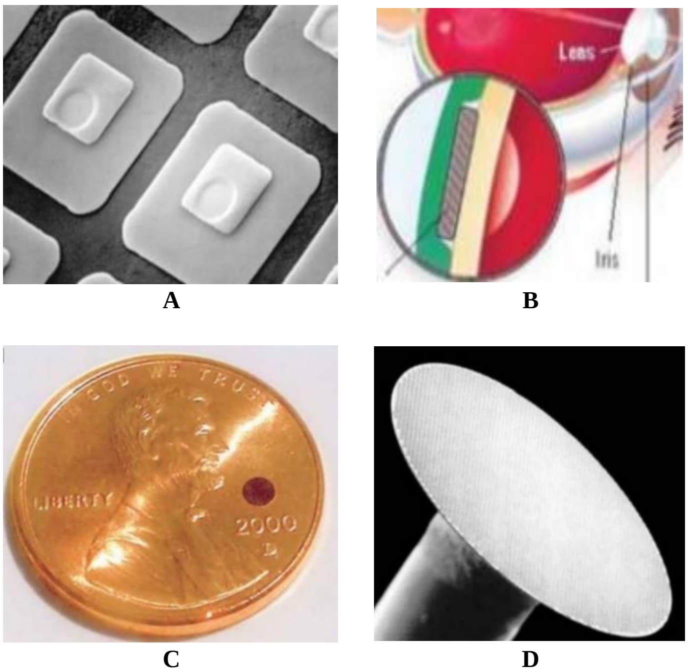

Figure 43. (A) artificial silicon retina chip shown relative to the size of a penny; (**(B)** 26X) in low-power scanning electron microscopic view; (**(C)** 1150X) as individual pixels; and **(D)** as positioned in the subretinal location. Reprinted with permission from the American Medical Association. 24 All rights reserved[9].

4.4.2. Advanced driver assistance system

Advanced Driver Assistance Systems (ADAS) currently on the market are performs specific functions such as lane departure warning (LDW), collision warning or high beam assist[14,15]. The reason why ADAS has been slow to enter the market is that there is still a lack of cost-effective solutions that would allow for broad market penetration and increased penetration, increasing the number of sensors and supported safety features[14]. For example, an LDW system is provided in 5 series and 6 series BMW to be an optical device[16]. However, although the high price is acceptable for vehicles in the higher price segment vehicles is acceptable, but not for lower priced and economical vehicles[14]. An important part in the ADAS is the bio-inspired silicon retina imagers. The reason why using the silicon retina is its high resolution and high dynamic range. For example, temporal resolutions of the silicon retina can up to 1ms are achieved due to the low resolution and asynchronous transmission of AE from pixels where intensity changes occur. **Figure 5** on the right shows the speed of the silicon retinal imager compared to the monochrome camera (Basler A601f). The top image pair on the right shows the running LED mode at a frequency of 45 Hz. Both camera types recognize LED motion. The LED pattern in the bottom right image pair is at 450 Hz[8]. Silicon retina captures jump sequences of LEDs, but monochrome cameras cannot capture fast-moving patterns, so multiple LEDs can be seen in a single image[8]. Another benefit of the silicon retina is its high dynamic range of up to 120 dB under various lighting conditions, as shown on the left in **Figure 44**, the silicon retina sensor can recognize the hand clearly when moving a hand in front of the photoreceptor. The silicon retina is free-running and sends data only when intensity changes produce AE. The data sent by the silicon retina can be used to control the car to assist driver driving or help driver avoid dangerous condition. Furthermore, in the future, this system is also very suitable for the unmanned vehicle, the silicon retina can detect the speed of other cars and then output a signal, and this signal can be used to control the motion of the unmanned vehicle to ensure the safety of the passengers.

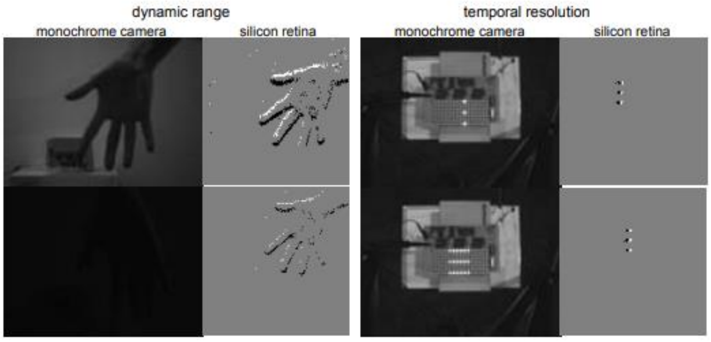

(a) **(b)**

Figure 44. (a) the top pair shows a hand moved under office illumination conditions (~1000/mm^2) and the lower pair on the left side shows the same scene with an illumination of ~5/mm^2; **(b)** the LED running speed in the top image pair is 45 Hz and in the lower image pair on the right 450 Hz[8].

4.4.3. Artificial robot

Visual movement is one of the sources of sensory information used on small robotic platforms[7]. In order to extract the motion information from the visual scene of the robot, a bio-inspired optical motion sensor, which is consisting of 20 × 20 continuous time CMOS silicon retina and DSP controller, is applied to the robotic system[7]. Motion information is calculated from the retinal output by implementing selected motion algorithms on the on-board DSPIC microcontroller. This setup allows experimentation with various 2D motion algorithms. It also facilitates the development of improved custom vision sensor chips for these applications. Using the included PC interface, algorithms can be quickly developed on the computer and then ported to the microcontroller of the robot. The microcontroller can control the behaviour of the robot. For example, the robot can capture moving objects within its own field of view and calculate them with different motion algorithms, and then output the relationship between robot and object motion[7]. Furthermore, other algorithms can be design to control the robot do different behaviours. To be more specific, an algorithm related to space can be used. This makes the silicon retina can also be applied to aerospace, it has the function of a human retina, which means that this eyeball can observe and convert the observed things into electrical signals, therefore this artificial intelligence retina can be used on robots, which can be transported to other planets through spaceships, and through its smart eyes help people explore the geological conditions of various planets. In the future, its application may be very widespread under the rapid development trend of AI, it may be used to detect undersea energy, could be used in unmanned aircraft, and unmanned cars to observe road conditions, and could be used to help residents to clean rooms.

5. Conclusion

In conclusion, the purpose of this project is to build some constraint-solving circuit on the PCB to detect motion in the x-axis and y-axis, which is one of the functions of the human retina. The whole project is divided into five steps, which include researching, simulating, building a cell on the breadboard and testing, presenting a cell on PCB and testing, printing more cells, and connecting all the cells. In the testing, the sinewaves are used as the inputs of the cell, and the frequencies of the output signals are becoming twice, which follows the calculations. Furthermore, when connecting the photoreceptor as the input, different motion types, which include moving fast (40 cm/s) or slow (20 cm/s), moving horizontally or vertically, and moving upward at an angle or downward at an angle, and the results are also basically following the analysis and the expected result read from the books or journals. Furthermore, silicon retina has a large market potential. The silicon retina can be applied in the medical area, advanced driving assistance systems, and artificial robots. Specifically, the Silicon retina can act as the eyes of a medical instrument to help doctors detect viruses and probe human organs or can be implanted into human eyes to help people whose vison is lost. Furthermore, the silicon retina can also act as the eyes of the car to help the driver to detect road conditions and thus assist the driver in effectively avoiding danger. Finally, the silicon retina can act as the eyes of the robot to help scientists explore the sea or aerospace. Thirdly, according to the above nearly 20 years of literature, people's exploration of the silicon retina is more and more extensive, more and more in-depth, and the development of the silicon retina has reached a very mature stage. The literature reviews are including the constraint-solving circuit, 1 kHz 2D visual motion sensor, bio-inspired stereo vision system with silicon retina imagers, artificial silicon retina for patients with retinitis pigmentosa, a programmable silicon retina with pattern recognition, and event-based camera. Finally, through this project, the knowledge related to advanced technology including integrated circuits, intelligent medical machines, driverless cars, and intelligent robots has been learned.

In the future, this system can be improved in that different speeds produce different output signals, which is not intuitive enough, thus an upper computer can be added to process and calculate the output signal, and then display the velocity in m/s.

Author contributions

Conceptualization, ZL and TJ; methodology, ZL; software, ZL; validation, TJ; formal analysis, ZL; investigation, ZL and TJ; resources, ZL and TJ; data curation, ZL and TJ; writing—original draft preparation, ZL; writing—review and editing, ZL and TJ; visualization, ZL and TJ; supervision, TJ; project administration, ZL and TJ; funding acquisition, ZL. All authors have read and agreed to the published version of the manuscript.

Conflict of interest

The authors declare no conflict of interest.

References

1. Teufl W, Miezal M, Taetz B, et al. P 052—Detection of lower extremity asymmetries in slow and dynamic bilateral tasks. Inertial Sensor system vs Optical Motion Capture System. Gait & Posture. 2022, 95: 219-220. doi: 10.1016/j.gaitpost.2018.06.205

2. Mahowald M. An Analog VLSI System for Stereoscopic Vision. Springer US; 1994. doi: 10.1007/978-1-4615-2724-4
3. Bonsor K. How artificial vision work. Available online: https://science.howstuffworks.com/innovation/everyday-innovations/artificial-vision3.htm (accessed on 10 May 2023).
4. Murakami I. The aperture problem in egocentric motion. Trends in Neurosciences. 2004, 27(4): 174-177. doi: 10.1016/j.tins.2004.01.009
5. Mead C. Analog VLSL and neural systems. California Institute of Technology Press. 1989.
6. ACTE. Using Schmitt Triggers for Low Slew-Rate Input. Available online: https://www.microsemi.com/document-portal/doc_view/130021-ac161-using-schmitt-triggers-for-low-slew-rate-input-app-note (accessed on 20 November 2002).
7. Liu SC, Yang M, Steiner A, et al. 1 kHz 2D Visual Motion Sensor Using Silicon Retina Optical Sensor and DSP Microcontroller. IEEE Transactions on Biomedical Circuits and Systems. 2015, 9(2): 207-216. doi: 10.1109/tbcas.2015.2414881
8. Kogler J, Sulzbachner C, Kubinger W. Bio-inspired Stereo Vision System with Silicon Retina Imagers. Computer Vision Systems. Published online 2009: 174-183. doi: 10.1007/978-3-642-04667-4_18
9. Chow AF, Bittner AK, Pardue MT. The artificial silicon retina in retinitis pigmentosa patients (an American Ophthalmological Association Thesis). Transactions of the American Ophthalmological Society. 2010.
10. Voon LFLY, Cathebras G, Bellach B, et al. Silicon retina for real-time pattern recognition. Blouke MM, Canosa J, Sampat N, eds. Sensors and Camera Systems for Scientific, Industrial, and Digital Photography Applications II. Published online May 15, 2001. doi: 10.1117/12.426951
11. Khan N, Martini MG. Bandwidth Modeling of Silicon Retinas for Next Generation Visual Sensor Networks. Sensors. 2019, 19(8): 1751. doi: 10.3390/s19081751
12. Simonite T. After silicon. New Scientist. 2006, 192(2578): 80. doi: 10.1016/s0262-4079(06)61152-4
13. Venkataraman S, Haftka RT. Structural optimization complexity: what has Moore's law done for us? Structural and Multidisciplinary Optimization. 2004, 28(6): 375-387. doi: 10.1007/s00158-004-0415-y
14. Navarro J, Mars F, Young MS. Lateral control assistance in car driving: classification, review and future prospects. IET Intelligent Transport Systems. 2011, 5(3): 207. doi: 10.1049/iet-its.2010.0087
15. Hamid UZA, Pushkin K, Zamzuri H, et al. Current Collision Mitigation Technologies for Advanced Driver Assistance Systems—A Survey. 2016.
16. Nica G. BMW Lane Departure Warning system to get an update this summer. Available online: https://www.bmwblog.com/2021/05/27/bmw-lane-departure-warning-system-to-get-an-update-this-summer/ (accessed on 27 March 2021).